



<b>Publication Year</b>	2010
<b>Acceptance in OA @INAF</b>	2024-02-22T09:43:43Z
<b>Title</b>	The AGILE silicon tracker: Pre-launch and in-flight configuration
<b>Authors</b>	BULGARELLI, ANDREA; ARGAN, ANDREA; Barbiellini, G.; Basset, M.; Chen, A.; et al.
<b>DOI</b>	10.1016/j.nima.2009.12.051
<b>Handle</b>	<a href="http://hdl.handle.net/20.500.12386/34808">http://hdl.handle.net/20.500.12386/34808</a>
<b>Journal</b>	NUCLEAR INSTRUMENTS & METHODS IN PHYSICS RESEARCH. SECTION A, ACCELERATORS, SPECTROMETERS, DETECTORS AND ASSOCIATED EQUIPMENT
<b>Number</b>	614

# The AGILE Silicon Tracker: pre-launch and in-flight configuration

A. Bulgarelli<sup>a,\*</sup> A. Argan<sup>b</sup> G. Barbiellini<sup>d</sup> M. Basset<sup>d</sup>  
A. Chen<sup>c</sup> G. Di Cocco<sup>a</sup> L. Foggetta<sup>g</sup> F. Gianotti<sup>a</sup> A. Giuliani<sup>c</sup>  
F. Longo<sup>d</sup> S. Mereghetti<sup>c</sup> F. Monzani<sup>e</sup> L. Nicolini<sup>e</sup> R. Pavese<sup>e</sup>  
A. Pellizzoni<sup>f</sup> C. Pontoni<sup>i</sup> M. Prest<sup>g</sup> G. Pucella<sup>b</sup> M. Tavani<sup>b</sup>  
M. Trifoglio<sup>a</sup> A. Trois<sup>b</sup> E. Vallazza<sup>d</sup> S. Vercellone<sup>j</sup>

<sup>a</sup>*INAF-IASF Bologna, Via P. Gobetti 101, I-40129 Bologna, Italy*

<sup>b</sup>*INAF/IASF-Roma, Via del Fosso del Cavaliere 100, I-00133 Roma, Italy*

<sup>c</sup>*INAF/IASF-Milano, Via E. Bassini 15, I-20133 Milano, Italy*

<sup>d</sup>*Dip. di Fisica and INFN Trieste, Via Valerio 2, I-34127 Trieste, Italy*

<sup>e</sup>*Tales Alenia Space Italia, Vimodrone (MI), Italy*

<sup>f</sup>*INAF-Osservatorio Astronomico di Cagliari, localita' Poggio dei Pini, strada 54,  
I-09012 Capoterra, Italy*

<sup>g</sup>*Dip. di Fisica e Matematica and INFN Milano Bicocca, Univ. dell'Insubria, Via  
Valleggio 11, I-22100 Como, Italy*

<sup>h</sup>*Dip. di Fisica, Univ. "Tor Vergata", Via della Ricerca Scientifica 1, I-00133  
Roma, Italy*

<sup>i</sup>*Altran, Via Benedetto Croce 35/37, I-56100 Pisa, Italy*

<sup>j</sup>*INAF/IASF Palermo, Via Ugo La Malfa 153, I-90146 Palermo, Italy*

---

## 1 Introduction

AGILE (Astrorivelatore Gamma ad Immagini LEggero - Light Imager for Gamma-ray Astrophysics) is a scientific mission of the Italian Space Agency (ASI). The AGILE payload [1] is composed of three detectors: (1) a Tungsten-Silicon Tracker (ST) ([2]-[3]) with a large field of view (about 60°), a good time sensitivity and angular resolution; (2) a Silicon based X-ray detector, Super-AGILE (SA) [4], for imaging in the 18-60 keV energy range, and (3) a CsI(Tl)

---

\* Corresponding author.

*Email address:* bulgarelli@iasfbo.inaf.it (A. Bulgarelli).

8 Mini-Calorimeter (MCAL) [5] that detects gamma-rays or particle energy de-  
9 posits between 300 keV and 100 MeV. The instrument is surrounded by an  
10 anti-coincidence (AC) system [6] of plastic scintillators for the rejection of  
11 charged particles. ST, MCAL and AC form the so called Gamma-Ray Imag-  
12 ing Detector (GRID) for observations in the 30 MeV-50 GeV gamma energy  
13 range. The introduction of the most recent detector technologies in the con-  
14 struction of AGILE brings to the realization of a very light payload (100 kg)  
15 with an effective area adequate to produce new important scientific results.  
16 AGILE was successfully launched by the Indian PSLV C8 rocket from the  
17 Sriharikota base on April 23rd 2007, in a quasi-equatorial orbit with an in-  
18 clination of  $2.5^\circ$ . The satellite in-orbit commissioning phase was carried out  
19 in the period May-June 2007. The scientific verification phase and scientific  
20 calibration (based on the Vela and Crab pulsars) were carried out during the  
21 period July-November 2007. The nominal scientific observation phase (AGILE  
22 Cycle-1, AO-1) started on December 1st, 2007.

23 In this paper we present the main results concerning the noise characterization  
24 and the front-end configuration of the Silicon Tracker. In particular, this work  
25 covers the configuration activities performed during the AIV (Assembly, Inte-  
26 gration and Verification) phase of the Silicon Tracker, and during the in-flight  
27 commissioning phase. The main purpose of these activities was to reach an  
28 optimal ST efficiency.

29 The activities performed during the assembly phase of the modules of the  
30 AGILE Silicon Tracker are reported in [7].

31 The paper is organized as follows. The Silicon Tracker is described in Section  
32 2 while Section 3 is devoted to the description of the on-board logic of the  
33 front-end for the determination of a GRID event cluster. Section 4 is dedi-  
34 cated to the identification procedure of the **anomalous** strips used during  
35 the assembly phase of the Silicon Tracker and Section 5 describes the param-  
36 eters characterizing the noise. Section 6 reports some considerations about the  
37 concept of floating strip and the definition of the ST efficiency. The GRID  
38 clusters, the determination of the noisy strips and the characterization of the  
39 noise are the main tools used to **optimize** the ST efficiency, that is the final  
40 goal of this work, as described in Section 7. Sections 8-9 report the results  
41 obtained during the pre-launch AIV and in-flight commissioning phases.

## 42 **2 The Silicon Tracker**

43 The main purpose of the Silicon Tracker (Figure 1) is to provide a compact  
44 imager for gamma-ray photons of energy above 30 MeV. The Tracker plays  
45 two roles at the same time: it converts the gamma-rays in heavy-Z material  
46 layers ( $245 \mu\text{m}$  of Tungsten,  $0.07 X_0$ ), where the photon interacts producing

47 an electron/positron pair (that are MIPs, Minimum Ionizing **Particles** corre-  
48 sponding to a most probable value of 110 keV) **deposited energy per layer**  
49 in the detector, and records the electron/positron tracks by a sophisticated  
50 combination of Silicon microstrip detectors and associated readout.



Fig. 1. *Photo of the tracker before the assembly of the 2 front-end boards (June 2005).*

51 A GRID event is a collection of all the electron/positron interactions into the  
52 microstrips of the silicon detector (each interaction generates a *cluster* that is  
53 a group of neighbouring strips collecting the charge deposited by the particle,  
54 see Section 3.3) together with the energy deposit in the MCAL bars and the  
55 information from the AC plastic scintillators (used as veto logic). A complete  
56 representation of the event topology allows the reconstruction of the incoming  
57 direction and energy of the  $\gamma$ -ray. A representation of a typical grid event is  
58 reported in Figure 2.

59 The Silicon Tracker [3] consists of 12 *planes*, each of them made of two layers  
60 of 16 single-sided, AC-coupled, 410  $\mu\text{m}$  thick,  $9.5 \times 9.5 \text{ cm}^2$  silicon detectors.  
61 The 16 detectors of each plane side (*view*) are grouped in 4 *ladders* each one  
62 consisting of 4 detectors wire bonded one after the other along the direction  
63 of the strips. The two views of the plane are organized in a *X-Z* configura-  
64 tion. Figure 3 presents the reference system and the numbering and naming  
65 conventions of the Silicon Tracker used in this paper.

66 The physical strip pitch is 121  $\mu\text{m}$  while the readout one is 242  $\mu\text{m}$ : this  
67 “floating strip” scheme allows to read one strip every two thus decreasing the  
68 number of readout channels (and thus decreasing the power consumption of  
69 the instrument) while maintaining an excellent spatial resolution. Each ladder  
70 has 384 readout channels. The name “strip” throughout the paper refers to a

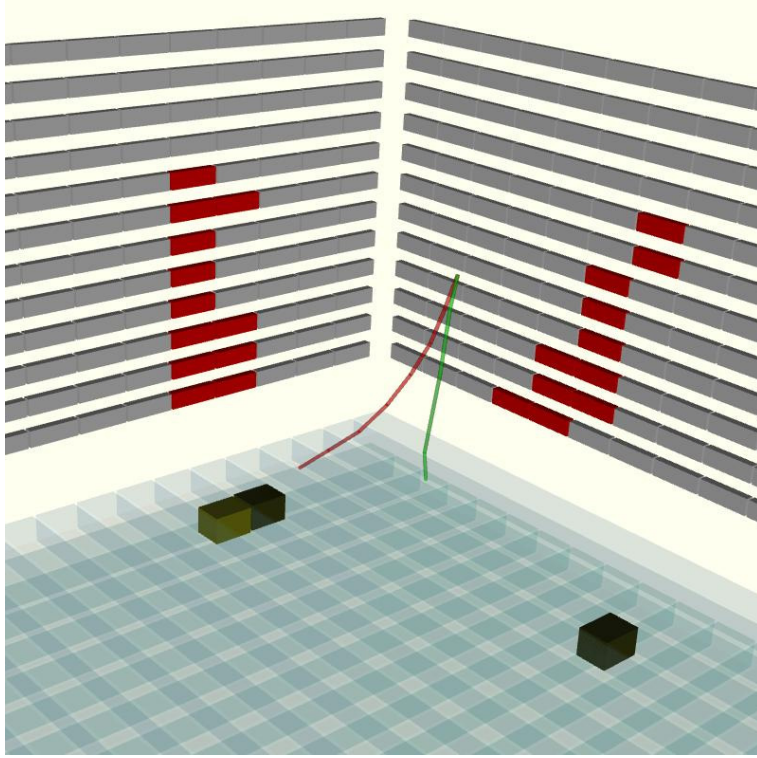


Fig. 2. A  $\gamma$ -ray event acquired in space **with a reconstructed energy of  $\sim 100$  MeV**. Gray boxes represent the ASICs and they are coloured in red if they have fired, **dark-yellow boxes mark the hits of the event into the MCAL** (the MCAL bars are cyan). The red and green lines are the reconstructed tracks (and thus the topology of the event) of the electron and the positron with a Kalman filtering technique.

71 readout strip unless otherwise indicated; “strip” and “channel” are equivalent.  
 72 The readout ASIC is the TAA1 (Gamma Medica - IDEAS), a mixed analog-  
 73 digital, low noise, self-triggering ASIC used in a very low power configuration  
 74 ( $< 400 \mu\text{W}/\text{channel}$ ) with full analog readout. More details are reported in  
 75 [2]. Each ASIC has 128 identical channels, containing a folded cascode pre-  
 76 amplifier, a CR-RC shaper, a discriminator (with a threshold chosen by the  
 77 user and a 3 bit trim DAC per channel for the fine setting) and a sample&hold  
 78 circuit. The readout is a multiplexed one, with a clock maximum frequency of  
 79 10 MHz; the value chosen for the tracker is 3.5 MHz, meaning that the time  
 80 needed to read one single ladder (that is 384 channels) is  $109.7 \mu\text{s}$ . The total  
 81 number of ASICs of the ST is 288, 24 ASICs for each plane.

82 **Latch-up events and single event effects have been considered in the**  
 83 **design of the electronics. Tests have been performed at the INFN**  
 84 **Laboratories of Legnaro with ions to understand the behaviour of**  
 85 **the ASIC. In the final design, care has been taken to prevent the**  
 86 **single event effects with a constant check of the trigger mask and**  
 87 **the latch-up problem with control and recovery circuits.**

88 The 12 planes of the Silicon Tracker are organized in 13 trays (as indicated on  
 89 the right of Figure 3) with a pitch of 1.9 cm. Each tray consists of a 12 mm

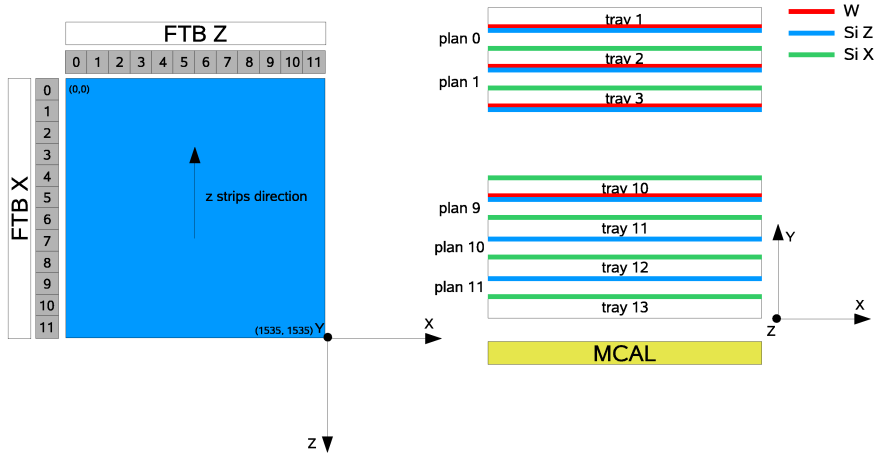


Fig. 3. The reference system of the Silicon Tracker used in this paper. On the left a logical view of a single plane is shown: the gray boxes are the readout ASICs, the numbers into the blue plan represent the numbering convention used for the strips. A plan is composed of a Z view (blue, shown in the scheme) and a X view. The Y direction is oriented to the top of the ST. On the right side the trays and the planes are shown. The red box is the W layer, the blue box represents the Silicon views with the strips along the Z direction and the green box shows the Silicon views with the strips along the X direction. The elements are not in scale.

90 core of aluminum honeycomb covered on both sides by a 0.5 mm carbon fiber  
 91 layer. The first 10 trays are equipped with a tungsten layer 245  $\mu\text{m}$  thick  
 92 glued on the bottom side of the tray itself and with the same area of the  
 93 silicon detectors. The overall on-axis ST radiation length is  $0.8 X_0$ <sup>1</sup>; the  
 94 silicon detector features allow to reach a spatial resolution of 40  $\mu\text{m}$  over a  
 95 wide range of incidence angles and an energy resolution (when working in the  
 96 GRID configuration mode) at 400 MeV of  $\frac{\Delta E}{E} \sim 1$ . The Silicon Tracker has  
 97 36 864 readout channels, and is logically and physically divided in 2 sides ( a  
 98 side is a collection of all the views with the same strip **direction**), called **X**  
 99 **and Z**, each one controlled by a dedicated front-end board (*FTB*, Frontend  
 100 and Trigger Board, [8]). Each FTB is composed of 6 *FEBs* (FrontEnd Board)  
 101 and each FEB controls 2 views of the same type. The FTB has to generate  
 102 the voltages needed to operate the ASICs ( $\pm 2$  V) and the bias voltage for the  
 103 silicon detectors, to set the threshold value, to manage the trigger signals and  
 104 the readout phase. The analog signals managed by the FEBs are Analog to  
 105 Digital converted and hardware processed by 3 PDHU (Payload Data Handling  
 106 Unit, see [9]) boards<sup>2</sup>. The silicon detectors have been manufactured on **six**  
 107 **wafers with resistivity above 4  $k\Omega\text{-cm}$** ; the corresponding full depletion

<sup>1</sup> There are 10 layers of W, each one of 0.07  $X_0$  radiation length, and 24 layers of Si, each one of 0.0410 cm. With the Si layers we obtain 0.1  $X_0$  radiation length.

<sup>2</sup> FTBs and PDHU have been designed by Thales Alenia Space (formerly Laben).

108 voltage ranges between 25 and 45 V and the bias voltage used on the satellite  
109 is 50 V.

110 The total height including the active elements is  $\sim 21$  cm and therefore the  
111 tracker is the lightest and most compact  $\gamma$ -ray imager sent in orbit.

### 112 3 ST front-end characterization

#### 113 3.1 Electronic Noise

114 The overall noise of each ladder has two components (see [2]):

- 115 • the intrinsic random noise, **characterizing** each floating or readout strip,  
116 whose single components are the ones listed below:
  - 117 · the leakage current;
  - 118 · the polarization resistors;
  - 119 · the resistance of the metal strip;
  - 120 · the TAA1 readout ASIC.

121 The estimated *Equivalent Noise Charge* (ENC) is of the order of 800  
122 electrons with the main contributions coming from the ASIC and the po-  
123 larization resistor of the detector.

- 124 • the common mode (CM), that characterizes each ASIC, which is given by  
125 the fluctuation of all the channels at the same time mainly because of the  
126 pickup on the bias voltage.

127 The expected noise for each ladder is the sum in quadrature of the two com-  
128 ponents.

129 As far as the grounding of the detector is concerned, all the power supplies  
130 have a common return defined at the level of the PDHU. This common return  
131 is the general ground of the system . This solution has been verified in terms  
132 of noise to check it did not deteriorate the performances.

133 A too high CM could prevent the possibility of setting the trigger threshold at  
134  $1/4$  of a MIP, that is the optimal value as specified in Section 6, **thus reducing**  
135 the detector trigger efficiency. In particular, with a too high threshold the  
136 floating strip could be lost. The CM has to be computed for each event to  
137 be subtracted together with the pedestal from the raw data, an operation  
138 performed by the FTB. For each ASIC  $j$  the CM component is calculated as

$$CM_j = \frac{\sum_{i=1}^N (raw_{ji} - ped_{ji})}{N_j} \quad (1)$$

139 where  $raw_{ji}$  is the raw content of the readout channel of the strip  $i$  in ADC  
140 counts,  $ped_{ji}$  is the channel pedestal (see Section 3.2) and  $N_j$  is the number  
141 of the ASIC good strips (noisy or dead strips are excluded).

### 142 3.2 Pedestal calculation

143 The pedestal of a channel is its baseline level when no signal is present.  
144 An on board procedure, activated by means of a dedicated telecommand,  
145 has been implemented for the pedestal calculation: the ASICs are divided in  
146 columns (corresponding to the first, second and so on ladders of each view);  
147 when the procedure starts each column is readout for 64 times generating  
148 random triggers and the values are stored on-board. The following quantities  
149 are then calculated, where  $j$  is the ASIC index and  $i$  is the strip index related  
150 to that ASIC:

- 151 • the mean value of each strip (36 864 values),  $ped_{ji}$ ;
- 152 • the rms value of each strip (36 864 values),  $rms_{ji}$ ;
- 153 • the common mode of each ASIC (288 values, one for each ASIC),  $CM_j$ , as  
154 reported in Equation 1.

155 In Figure 4 the histograms of the mean and rms (before the common mode  
156 subtraction) values and the common mode rms for each ASIC are presented.  
157 Given the overall noise rms is of the order of 30 ADC counts, and the common  
158 mode value is of the order of 6, the common mode contribution to the noise is  
159 **practically negligible**. Figure 5 shows the pedestal mean and rms for each  
160 strip of a single ASIC.

### 161 3.3 Determination of a cluster in an event

162 A cluster is a set of contiguous strips registering the passage of a particle. The  
163 following on-board algorithm is used to identify the clusters:

- 164 • the TAA1 ASIC contains a threshold discriminator per read-out channel.  
165 If the value of the charge of a strip is above this threshold (called *FTB*  
166 *threshold*) a *trigger signal* is generated (which is the OR of all the 128  
167 channels of a TAA1). This signal starts a level 1 trigger algorithm (see [3]),  
168 that requires a signal in at least three out of four contiguous tracker planes,  
169 and a proper combination of fired AC panels;
- 170 • if the previous level 1 trigger is passed, a *hold signal* is generated and an  
171 intermediate level 1.5 trigger (see [3] for details) evaluates the event topology  
172 defined by the distribution of the fired ASICs with respect to the fired AC  
173 panels;



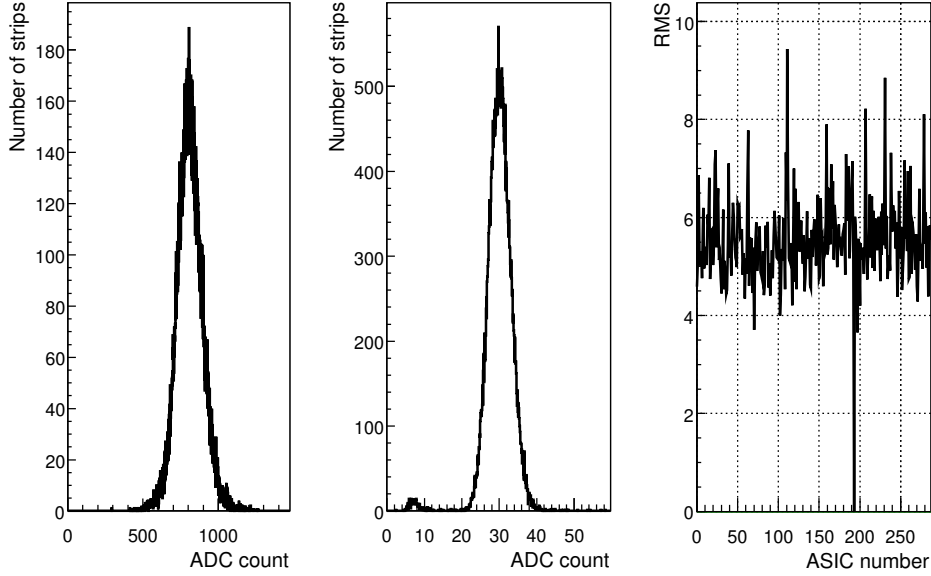


Fig. 4. Histogram of the pedestal mean ( $ped_{ji}$ ) and rms ( $rms_{ji}$ ) and plot of the common mode rms of each ASIC (the x axis reports the index of the ASIC). The small peak below 10 ADC counts in the rms distribution is related to dead channels where only CM noise is present. The common mode rms near 0 ADC counts is due to a dead ASIC.

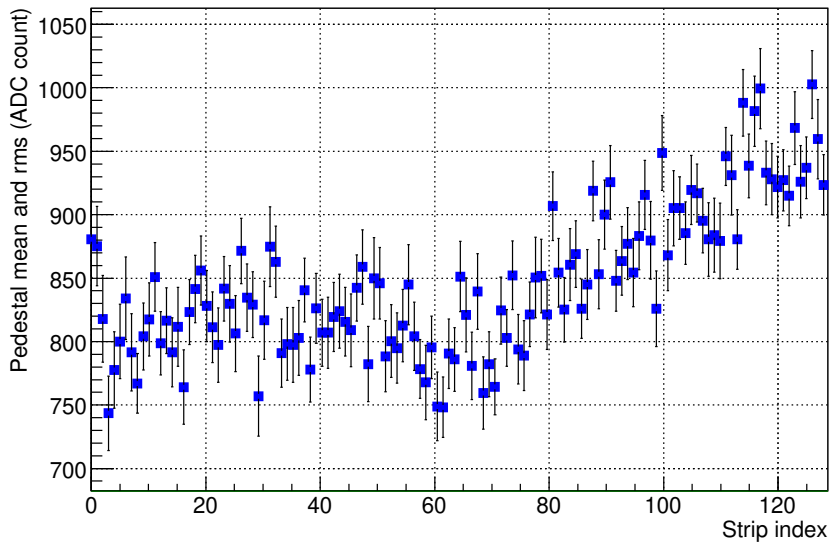


Fig. 5. Pedestal mean ( $ped_{ji}$ ) and rms ( $rms_{ji}$ ) of each strip of an ASIC.

- 174 • if the level 1.5 trigger is passed all the strips **with signal above the**  
 175 **threshold for the fired ASICs** are acquired and their collected charge  
 176 is converted **into** 12 bit digital values. To do this, the *front-end freeing*  
 177 procedure implements a sparse readout of the triggered strips by means of  
 178 a 5 MHz clock and the analog to digital converted values are saved in a

179 dedicated RAM;

180 • at this point, a *preprocessing procedure* starts:

181 • *raw data pre-analysis*: the pedestal and common mode values are sub-  
182 tracted; the pulse height of every strip  $i$  of ASIC  $j$  is thus defined as

$$C_{ji} = raw_{ji} - ped_{ji} - CM_j \quad (2)$$

183 • *zero suppression*: **each** strip with a value  $C_{ji}$  smaller than  $N_1$  times its  
184 rms is discarded. This reduces the data transfer to the PDHU. At the time  
185 of writing,  $N_1 = 3$  [2];

186 • *cluster identification*; this procedure starts after the preprocessing procedure  
187 and **contains** the following steps:

188 • in a group of contiguous strips at least one strip  $m$  should have a value  
189  $C_m > H_m$ , where  $H_m$  is  $N_2$  times the  $rms_m$  calculated with the pedestal  
190 procedure. At the time of writing,  $N_2 = 5$  [2];

191 • the **not suppressed** strips adjacent to the strip  $m$  are considered. This  
192 group of strips is called a cluster. If in this group there are two strips with  
193 a signal  $C$  larger than  $N_2$  times their rms noise and they are not adjacent  
194 to **one another**, two clusters are generated with a shared strip.

195 For each cluster the payload telemetry contains:

196 • the total charge (the sum of the charges of all the cluster strips);

197 • the total width (the number of strips) of the cluster;

198 • the charge of the 5 central strips of the cluster, reduced to 8 bits (the least  
199 significant bits are removed). In this paper the central strip is called  $C_3$ , the  
200 left side strips are called  $C_1$  and  $C_2$ , and the right side strips are called  $C_4$   
201 and  $C_5$ .

202 In addition, the following data are acquired for a full representation of the  
203 GRID event:

204 • the time of the event;

205 • the energy deposited in each Mini-Calorimeter bar;

206 • the configuration of the fired AC panels;

207 • the extra fired ASICs index: for each view of the Silicon Tracker the maxi-  
208 mum number of triggered ASICs that can be acquired is 8. If more than 8  
209 ASICs trigger, only the indexes of the additional triggered ASICs are sent  
210 to ground with the telemetry. The ASICs are ordered according to their  
211 physical position: from the first tray on the top of ST to last tray at the  
212 bottom, and for each tray according with the index reported in Figure 3.

### 213 3.4 The GRID Operation mode

214 The PDHU provides three main working modes for the GRID subsystem:

- 215 1 *observation mode*: with this configuration the GRID subsystem is **ready**  
 216 to acquire photons in the 30 MeV-50 GeV energy band. A set of dif-  
 217 ferent on-board triggers (level 1 and level 1.5 hardware trigger, already  
 218 described in Section 3.3, and a level 2 software trigger, see [9]) enables the  
 219 discrimination of background events (mainly muons on ground or particles  
 220 in the AGILE Low Earth Orbit) from gamma-ray events. This is the  
 221 acquisition mode used during the calibration activities and in-flight. The  
 222 corresponding telemetry flow is indicated as 3901;
- 223 2 *physical calibration mode*: in this configuration mode only the first step of  
 224 level 1 trigger that requires a signal in at least three out of four contiguous  
 225 tracker planes has been enabled. This data acquisition mode has been  
 226 used extensively during the various AIV activities. The corresponding  
 227 telemetry flow is indicated as 3902.
- 228 3 *electrical calibration mode*: this mode is used to check the behaviour (in  
 229 terms of gain and stability) of each single strip in test mode; all the strips  
 230 except one are disabled and a pulse with a variable amplitude is injected  
 231 into the preamplifier input 64 times, after having set a proper threshold.  
 232 The output is the number of times the strip has triggered. The procedure  
 233 is repeated for every strip. The corresponding telemetry flow is indicated  
 234 as 3904.

#### 235 4 Procedure for the identification of anomalous strips

236 The procedure for the identification of anomalous strips has been defined  
 237 during the assembly of the Silicon Tracker performed at Mipot S.p.A. <sup>3</sup> by  
 238 the INFN Trieste team.

239 A channel is considered *anomalous* or *bad* from the point of view of the noise  
 240 if the noise level is too low (low or dead channel) or too high (noisy channel).  
 241 It can be observed that, excluding the anomalous channels, the plot of the noise  
 242 versus the channel number is a function that has a continuous component. This  
 243 is probably due to the fact that the physical properties that have influence on  
 244 the noise level vary continuously (e.g. across the strips of the silicon detectors).  
 245 An example of this behaviour can be seen in Figure 6, where the noise of the  
 246 384 channels of a unit of electronic readout (a PCB with three ASICs, not  
 247 connected to the silicon detectors) is shown: **being the traces of the PCB**  
 248 **not connected to the corresponding strips on the silicon**, the noise  
 249 level is mainly determined by the different length of the strips on the board,  
 250 that vary slightly from a channel to the next **one**.

251 For this reason, the procedure starts with a fit of the noise level versus the  
 252 channel number with a curve of the second order; a different curve is obtained  
 253 for each ASIC. Then, a sort of level of anomaly for each channel ( $ANOM_n$ )

<sup>3</sup> Mipot S.p.A., Via Corona 5, Cormons (GO, Italy); <http://www.mipot.com>

254 is defined dividing the level of the noise of the single channel ( $rms_n$ ) by the  
 255 corresponding theoretical level calculated from the fit. In this way, a quite flat  
 256 function of the channel number is obtained, whose median is 1; a channel is  
 257 being defined bad considering how far its anomaly level is with respect to 1.  
 258 The noise level ( $rms_n$ ), which is the rms value of a set of measurements of the  
 259 pedestal acquired at different instants, has in turn a variance, that propagates  
 260 to the anomaly level. Hence, for each ASIC, the median, the lower quartile  $q_1$   
 261 and the upper quartile  $q_3$  of the set of the 128 anomaly levels in the ASIC  
 262 are calculated. Then, every single ( $ANOM_n$ ) is compared to  $q_1$  and to  $q_3$ :  
 263 the cut level is defined with the help of an arbitrary constant  $L$ , so that a  
 264 channel  $n$  is defined “low” or “dead” if  $ANOM_n < q_1^L$ , while it is “noisy” if  
 265  $ANOM_n > q_3^L$ . In the analysis, it has been chosen  $L = 15$ .  
 266 An example concerning one of the 24 views is presented in Figure 7; the data  
 267 shown in this picture refer to measurements acquired from a tray alone, not  
 268 assembled on the payload, shielded against EM interference, and connected to  
 269 a testbench electronic interface.

270 It has to be remarked that before every fit, the channels in the ASIC that  
 271 are clearly anomalous must be excluded from the fit algorithm, otherwise a  
 272 bad curve is obtained. The channels that are to be excluded from **the** fit are  
 273 determined by applying an algorithm similar to the one just described above,  
 274 except that the “fitting curve” is a flat line whose level is the median of the  
 275 ( $rms_n$ ) in the ASIC.

276 During the analysis, it has been noted that the noisy channels are better  
 277 highlighted after the common mode subtraction. Therefore, noise after the  
 278 common mode subtraction has been preferably used, instead of the raw rms,  
 279 to find the noisy channels, applying the same procedure described above.

280

## 281 5 Other quantities to characterize the GRID noise

282 **This section describes** the other quantities, in addition to those defined in  
 283 the pedestal calculation procedure (described in Section 3.2), that characterize  
 284 and optimize the overall GRID **noise and** efficiency.

### 285 5.1 Pull and SNR of a cluster

286 The pull [2] is defined as the ratio between the signal of the strip with the  
 287 maximum ( $C_3$ ) and its rms.

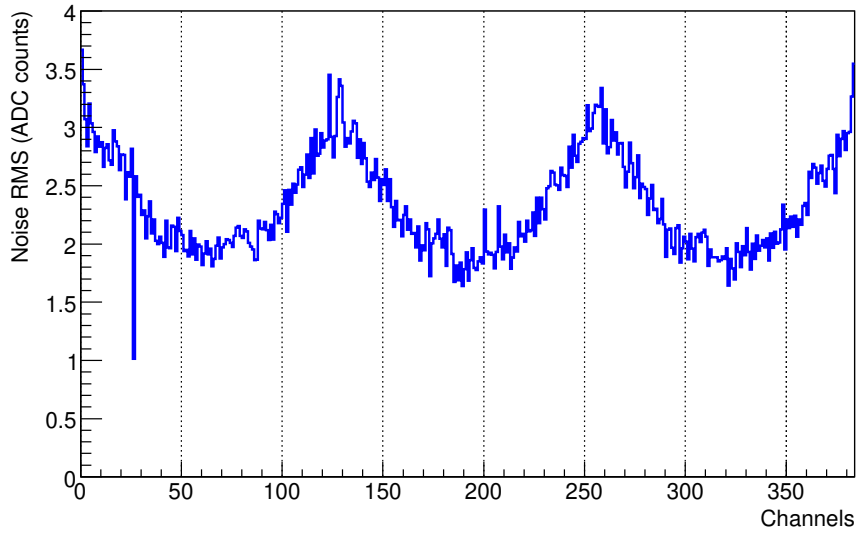


Fig. 6. Noise profile of the 384 channels of a PCB not connected to the silicon detectors. The typical shape of the profile is determined by the different length of the strips on the PCB that are connected to each channel of the ASIC. A dead channel can also be seen.

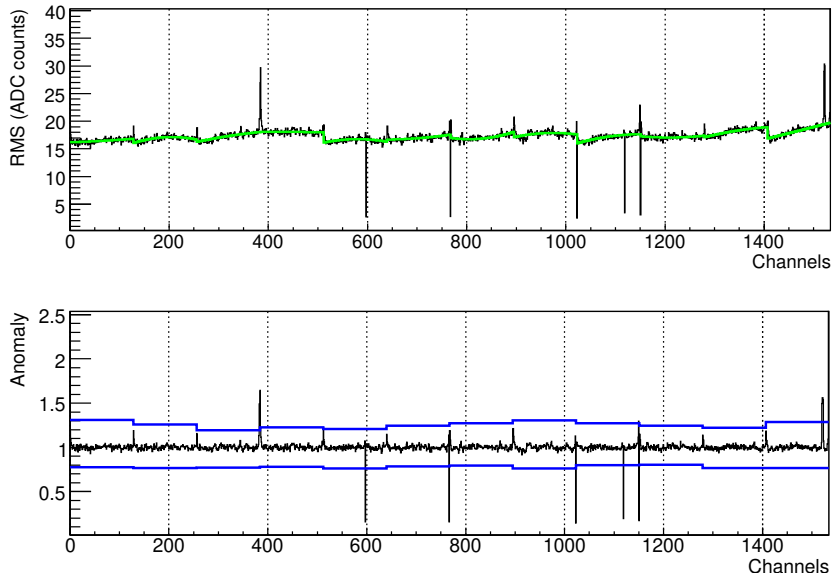


Fig. 7. Rms and anomaly level of the 1536 channels of an entire view (12 ASICs). In the upper plot, the parabolic fits of the ASICs can be seen; in the anomaly graph, the two cut levels for the evaluation of the low and of the noisy channels are also shown. Dead channels are 598, 768, 1024, 1120, 1152; noisy channels are 383-384, 1150, 1521 to 1523.

288 The signal/noise ratio (SNR) of a cluster is defined as

$$SNR = \frac{\sum_i C_i}{\sqrt{\frac{\sum_i rms_i^2}{N}}} \quad (3)$$

289 where the sum is performed over all the strips  $N$  in the cluster itself. Both  
 290 these quantities have been used for the characterization of the Silicon Tracker.  
 291 In particular, the peak of the pull (calculated as the most probable value of the  
 292 fit with a Landau [2]) and the on-axis pull (the pull of particles or converted  
 293  $\gamma$ -ray events **with incidence angle**  $< 5^\circ$ ) have been used for a check on the  
 294 threshold setting values  $N_1$  and  $N_2$  once the Silicon Tracker was integrated into  
 295 the spacecraft. In addition, the on-axis pull has been used for the evaluation  
 296 of the presence of events with particle crossing near the floating strip during  
 297 the various phases of the configuration (see Section 6).

## 298 5.2 Zero cluster events

299 During the AIV activities, it has been found that the generation of GRID  
 300 events with no clusters depends on the noise level of the Silicon Tracker itself.  
 301 When the level 1.5 trigger is passed, all the ASICs over threshold are acquired  
 302 and the preprocessing procedure is performed; during this procedure it is pos-  
 303 sible that all the ASICs are zero-suppressed but the on-board logic sends these  
 304 events to ground within telemetry all the same.

305 This generation of zero cluster events is due to the fact that if the system is  
 306 noisy the pedestal rms values are large and the two trigger levels can be passed  
 307 all the same; on the other hand, the procedure of the pedestal/common mode  
 308 subtraction and zero suppression eliminates all these clusters. For this reason  
 309 the number of zero cluster events has been used as a noise indicator during  
 310 the AIV and in-flight configuration of the Silicon Tracker front-end.

## 311 5.3 Extra-fired ASICs

312 As already stated, for each view of the Silicon Tracker the maximum number  
 313 of triggered ASICs that can be acquired is 8. If more than 8 ASICs trigger  
 314 (because of physics or because of the noise level of the detectors), only the  
 315 index of the additional triggered ASICs is sent to ground within the telemetry.  
 316 These ASICs are called *extra fired* and their number has been used as an  
 317 additional indicator of noise.

#### 318 5.4 Silicon Tracker rate-meters

319 The PDHU implements several rate-meters that can be used as indicators of  
320 the noise level of the system. In particular, the *ST rate-meters* are the OR  
321 of the trigger signals of all the TAA1 ASICs of a view (see Section 3.3). One  
322 rate-meter for each plane is generated, but only one view is sampled: the se-  
323 lection of the odd or even views is performed by means of a telecommand.  
324 Each rate-meter has an integration window of 16 s.

325

#### 326 5.5 Central strip charge

327 The distribution of the charge of the cluster central strip  $C_3$  can be used as  
328 indicator of the noise level of the Silicon Tracker. As reported in Section 8, the  
329 most probable value of the MIP charge is 630 ADC counts **for central strip**  
330  $C_3$ , with a typical distribution that can be fitted with a Landau function. For  
331 this reason the percentage of clusters with the central strip charge  $C_3 < 100$   
332 ADC counts has been evaluated, since this value is an indicator of a cluster  
333 triggered by noise.

### 334 6 Floating strip and efficiency measurement

335 The total charge collected by the readout strip depends on

- 336 • the diffusion during the charge collection;
- 337 • the capacitive charge coupling between the strips;
- 338 • the incidence angle of the incoming and secondary ionization particles.

339 As already stated, the AGILE Silicon Tracker is characterized by one float-  
340 ing strip between each readout strip. If a particle crosses the detector at the  
341 position of the floating strip, the charge is collected on this strip and induced  
342 on the nearby ones; capacitive charge division will then result in signals on  
343 more than one strip. Given the parameters of the detector strip (**such as**  
344 **width and pitch of implant strips and Al read-out electrodes**), when  
345 a particle crosses a floating strip, on each of the adjacent readout ones 38%  
346 of the produced charge is collected, as determined experimentally [3]. Such  
347 values are compatible with a 100% efficient detector if the trigger threshold  
348 is set at 1/4 of the charge released by a MIP crossing the silicon detector. A  
349 too high FTB threshold could reduce the detector efficiency preventing the  
350 readout strips to generate a trigger in case of an event on a floating strip.

351 If all the parameters are set correctly, the on-axis pull for the strip with the  
 352 maximum signal in the event shows clearly the presence of the floating strip  
 353 as presented in Figure 8, obtained with the Silicon Tracker in the final con-  
 354 figuration, already integrated in the spacecraft before the launch. The peak  
 355 on the left (whose most probable value is 10.6) corresponds to the case of the  
 356 particle crossing nearby a floating strip, while the peak on the right (with  
 357 a most probable value at 23.4) is the one of the readout strip collecting the  
 358 whole charge.

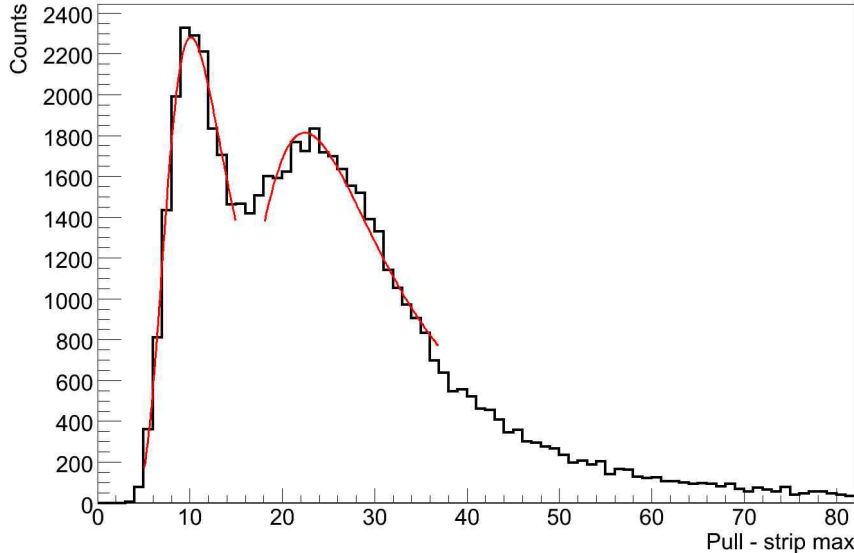


Fig. 8. *On-ground configuration: on-axis pull for the strip with the maximum with a FTB threshold set to 7 in physical calibration mode (data acquired on RUNID 11119). The peak on the left is due to the floating strip, while the peak on the right to the readout strip. The two peaks are fitted with a simplified Landau. The plot includes the data from all the ST planes.*

359 The easiest way to measure the plane efficiency is the following

$$eff(N) = N_s/N_t \quad (4)$$

360 where  $N_s$  is the number of GRID events with a signal (at least one cluster for  
 361 each plane) in the planes N-2, N-1, N, N+1, N+2 and  $N_t$  is the number of  
 362 GRID events with a signal (at least one cluster for each plane) in the planes N-  
 363 2, N-1, N+1, N+2. The ST efficiency is the mean value of the plane efficiencies.  
 364 The formula cannot be applied for planes 1, 2, 11 and 12, but due to the fact  
 365 that there is a difference between the efficiencies of the different planes of the  
 366 order of 1 – 2%, this formula has been used for the determination of the ST  
 367 efficiency.

368 The optimization of the ST efficiency was the main goal of the ST configura-



369 tion performed during the AIV and in-flight commissioning phases.

370

## 371 7 FTB threshold scan and strip mask definition

372 During the AIV activities several levels of the FTB threshold have been tested.  
373 All the tests have been performed with the same environmental conditions.  
374 For each threshold different strip masks have been chosen; in fact, the number  
375 and identity of noisy strips change as a function of the threshold and differ-  
376 ent masks of disabled strips have to be defined. This iterative procedure for  
377 the FTB threshold scan and noisy strip disabling has allowed the final con-  
378 figuration of the Tracker front-end; for each threshold the following steps are  
379 required:

380 • *First step:*

- 381 · a set of consecutive (typically 8-10) pedestal runs (telemetry type 3903)  
382 is performed allowing to create a first list of noisy strips resulting from  
383 the statistical analysis of the pedestals themselves (i.e. tagging individual  
384 strips displaying fluctuations **not compatible with those expected**  
385 **according to poisson statistics from average strip signal**);
- 386 · a second list is produced with the analysis of an electrical calibration  
387 (telemetry type 3904); the strips above a threshold (5 times the mean  
388 value of the number of triggers of all the strips of an ASIC) are selected.  
389 The digital value of the parameters used for electrical calibration are 1 for  
390 amplitude and 5 for threshold (see Section 3.4);
- 391 · These two lists are merged with a list of 242 noisy strips (about  $\sim 0.6\%$   
392 of total strips) identified during the Silicon Tracker assembly with the  
393 procedure described in Section 4.

394 • *Second step:* this first list is uploaded in the PDHU and an acquisition of  
395 GRID events in physical calibration mode (telemetry type 3902) is per-  
396 formed. Noisy strips are searched for in this data set: for each ASIC the  
397 mean  $\mu$  of the number of times  $\delta_i$  that a strip  $i$  is a center of a cluster is  
398 calculated. A strip  $i$  is noisy if  $\delta_i > \mu N$ . A typical value of  $N$  used during  
399 this analysis is 3; with this value a good equalization of the counts of each  
400 strip has been obtained. At the end of this procedure a new list is produced.

401 • *Third step:* the list is tested with a new physical calibration and the proce-  
402 dure is repeated if there are still noisy strips. The ST rate-meters are used  
403 as a quick look of the data quality of the configuration and the already de-  
404 scribed noise indicators (see Section 5) and the ST efficiency are evaluated.  
405 The procedure stops when good noise indicators have been obtained and  
406 a run of GRID observation (telemetry type 3901) is performed as the last  
407 check of the current configuration. This run allows to evaluate the efficiency  
408 and noise level of the system with the same parameters used in physical

409 calibration together with the topology of the acquired events.

410 Once this procedure is completed, the FTB threshold is changed and the  
411 process restarts.

412 The lower the FTB threshold, the higher the ST efficiency. The FTB threshold  
413 scan procedure stops when the ST noise becomes too high and too many strips  
414 (more than 6 – 7%) should be disabled.

415 The values of FTB thresholds reported in this paper are digital values without  
416 a direct correspondence with the MIP.

417 For each strip mask the following quantities have been used to decide if the  
418 current configuration is correct and the noise is under control:

- 419 • maximum peak of the pull and presence of the floating strip peak in the  
420 on-axis pull;
- 421 • SNR ratio;
- 422 • percentage of zero cluster events;
- 423 • percentage of extra-fired ASICs;
- 424 • ST rate-meters;
- 425 • counts of clusters with  $C_3 < 100$  ADC counts.

426 A configuration is good when the first 2 parameters of the list (in addition with  
427 the ST efficiency) have been maximized and the remaining **ones** minimized.  
428 In addition, the value of ST rate-meters should be uniform for each view.

429 In Table 1 the number of disabled strips for each configuration is reported. The  
430 configuration named 5 has been used during the GRID calibration performed  
431 in November 2005 at the INFN Laboratories of Frascati (Rome), while config-  
432 uration 6 was the on-board configuration selected before the launch campaign.  
433 Configurations 7 and 8 have been defined during the in-flight commissioning  
434 phase performed in May-June 2007.

Table 1  
*Number of disabled strips for each configuration.*

<b>Configuration</b>	<b>Nr of disabled</b>	<b>% of total</b>
<b>Name (Mask ID)</b>	<b>strips</b>	<b>strips</b>
5	1956	5.3
6	529	1.4
7	407	1.1
8	665	1.8

## 435 8 ST characterization at the end of the AIV activities

436 The ST final configuration is a trade-off between the noise level and the effi-  
 437 ciency of the Silicon Tracker and is the result of 597 runs in observation mode  
 438 (telemetry type 3901) and 996 runs in physical calibration mode (telemetry  
 439 type 3902) during the AIV activities. Each run is identified by its own RUNID  
 440 number in the AGILE test environment (see [11]-[14]). In the following, one  
 441 of the final runs is presented as an example (RUNID 11119). The main pa-  
 442 rameters of this final pre-flight configuration are the following:

- 443 • side X pull:  $16.7 \pm 0.2$
- 444 • side Z pull:  $16.2 \pm 0.2$
- 445 • events with less than 3 clusters: 1%
- 446 • clusters with less than 100 ADC counts for the central strip: 0%
- 447 • side X efficiency:  $95 \pm 2\%$
- 448 • side Z efficiency:  $97 \pm 2\%$

449 The strip mask used for this configuration is named 6 with 529 disabled strips.

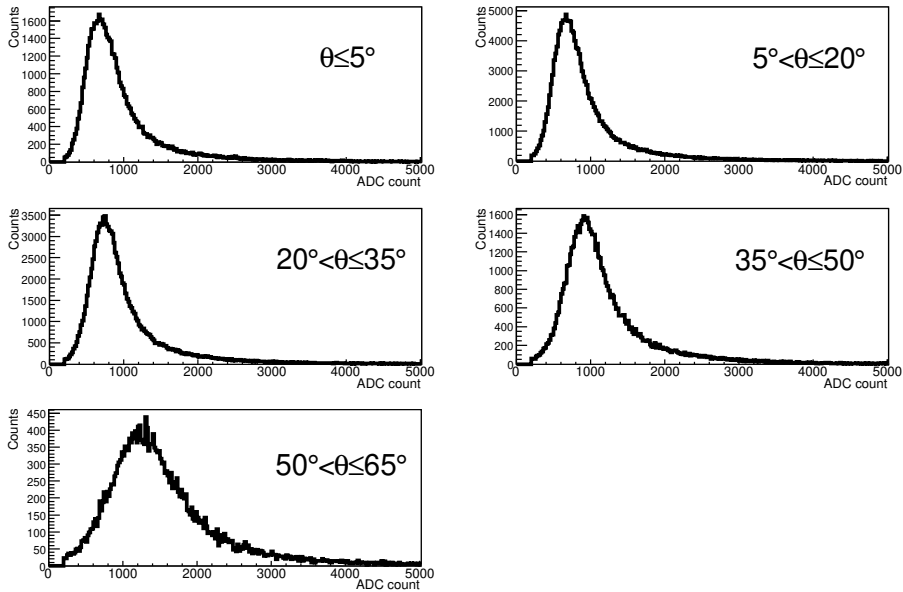


Fig. 9. *On-ground configuration: cluster total charge in ADC counts with the FTB threshold set to 7 and strip mask ID 6 in physical calibration mode for GRID events with different incidence angles  $\theta$ . Data acquired on RUNID 11119; the plots contain the data from all the ST planes.*

450 Figure 9 shows the total charge deposit in ADC counts of each cluster with  
 451 the FTB threshold set to 7 with data acquired in physical calibration mode.  
 452 Figure 10 presents the charge (in ADC counts) of the cluster central strip: for  
 453 near on-axis events it is possible to clearly distinguish the two peaks (first plot  
 454 at the upper left of the Figure) corresponding to the floating strip (peak on the

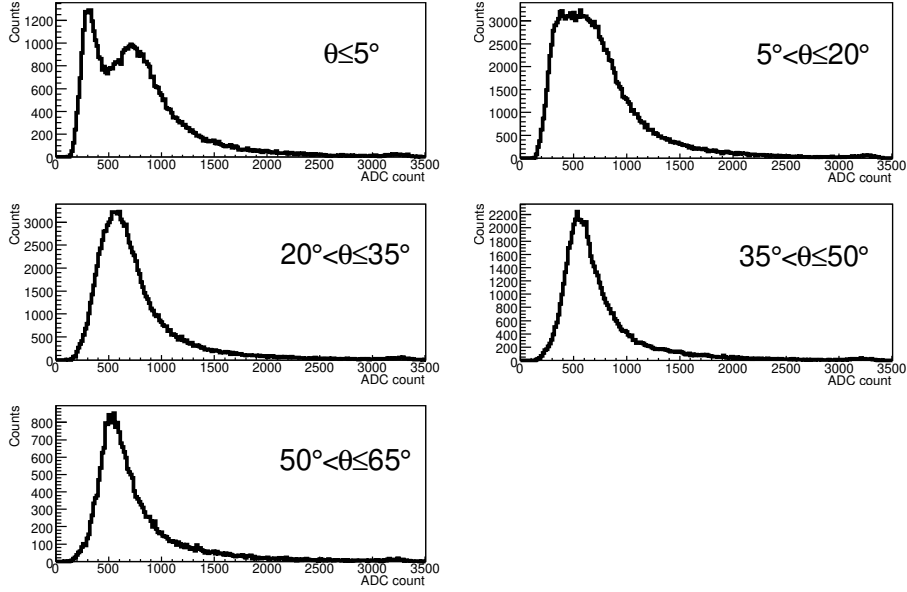


Fig. 10. *On-ground configuration: charge in ADC counts of the central strip  $C_3$  with the FTB threshold set to 7 and strip mask ID 6 in physical calibration mode for GRID events with different incidence angles  $\theta$ . In the first plot the peak on the left is due to the floating strip, the peak on the right to the readout one. Data acquired on RUNID 11119; the plots contain the data from all the ST planes.*

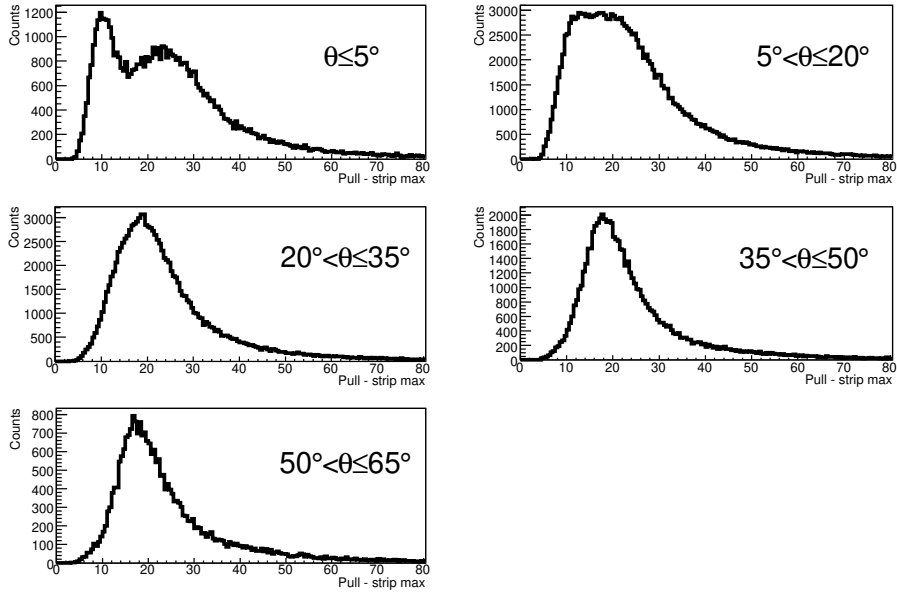


Fig. 11. *On-ground configuration: pull for the strip with the maximum signal in the event with the FTB threshold set to 7 and strip mask ID 6 in physical calibration mode for GRID events with different incidence angles  $\theta$ . Data acquired on RUNID 11119; the plots contain the data from all the ST planes.*

455 left) and to the readout one (peak on the right). The two peaks merge into one  
 456 for increasing incidence angles as a consequence of the charge signal spreading

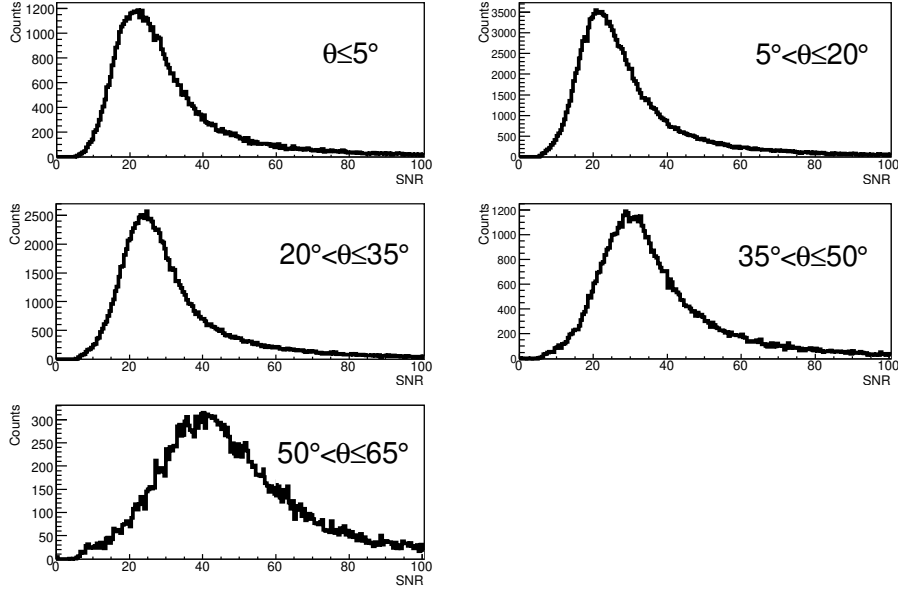


Fig. 12. *On-ground configuration: SNR with the FTB threshold set to 7 and strip mask ID 6 in physical calibration mode for GRID events with different incidence angles  $\theta$ . Data acquired on RUNID 11119; the plots contain the data from all the ST planes.*

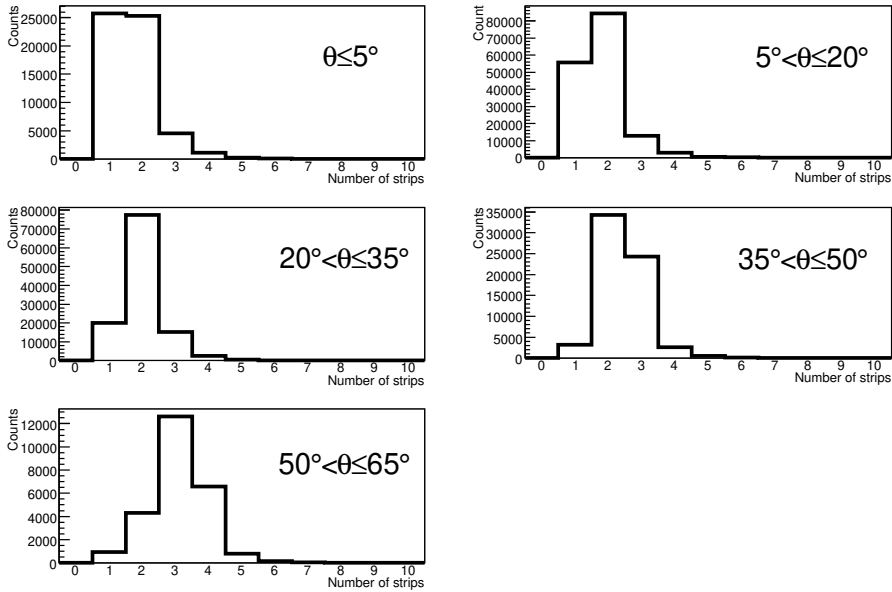


Fig. 13. *On-ground configuration: total width of the clusters with the FTB threshold set to 7 and strip mask ID 6 in physical calibration mode for GRID events with different incidence angles  $\theta$ . Data acquired on RUNID 11119; the plots contain the data from all the ST planes.*

457 over more strips for large inclinations. **Considering all inclinations** the  
 458 most probable value is about 630 ADC counts; this means that the conversion  
 459 factor between  $C_3$  (**ADC counts**) and MIP signal is about 0.174 keV / ADC

460 count.

461 Figure 11 shows the pull for different incidence angles of GRID events.

462 Figure 12 shows the SNR for different incidence angles and Figure 13 the total  
463 width of the clusters. This Figure demonstrates clearly why only 5 strips have  
464 been sent to telemetry.

## 465 9 The threshold scan during the in-flight configuration

466 During the in-flight configuration performed in the commissioning phase in  
467 May-June 2007 a scan of the FTB thresholds with the definition of new strip  
468 masks has been performed. The Silicon Tracker has been switched on the first  
469 time after the launch with a FTB threshold set to 20; the tests reported in  
470 Table 2 and Table 3 have been carried out after a verification that everything  
471 was working correctly.

472 Figures 14-17 report the on-axis pull for 3 values of the threshold (20, 6 and  
473 5) and for the chosen final configuration (FTB threshold set to 6 and strip  
474 mask definition identified as configuration 8).

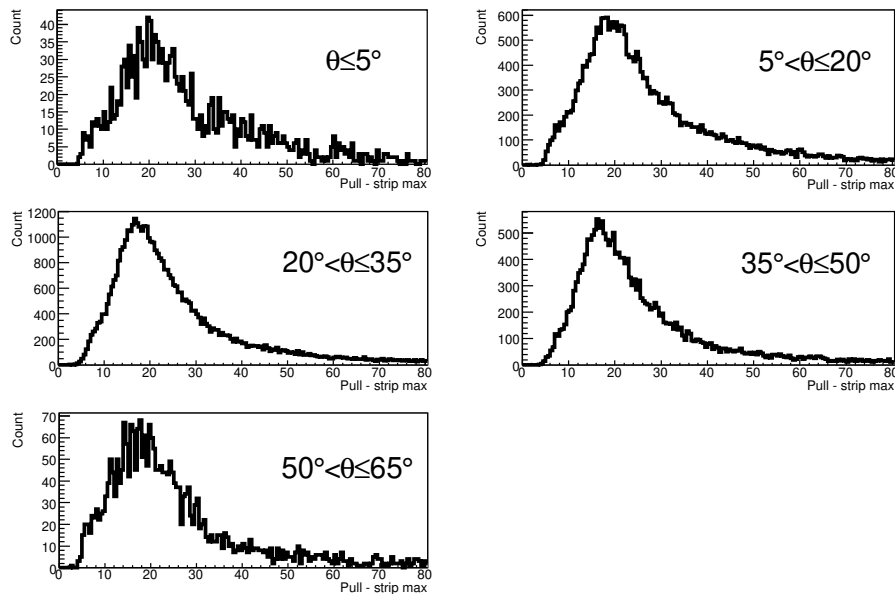


Fig. 14. *In-flight configuration: pull with the threshold set to 20 and strip mask ID 6 in physical calibration mode (data acquired with orbit 253) for GRID events with different incidence angles  $\theta$ . The plots contain the data from all the ST planes.*

475 Table 2 reports the noise and efficiency indicators in physical calibration mode  
476 and Table 3 in observation mode.

477 Figure 14 shows the pull of the first in-flight switch-on of the Silicon Tracker  
478 after the launch with the FTB threshold set to 20; as expected, the peak of

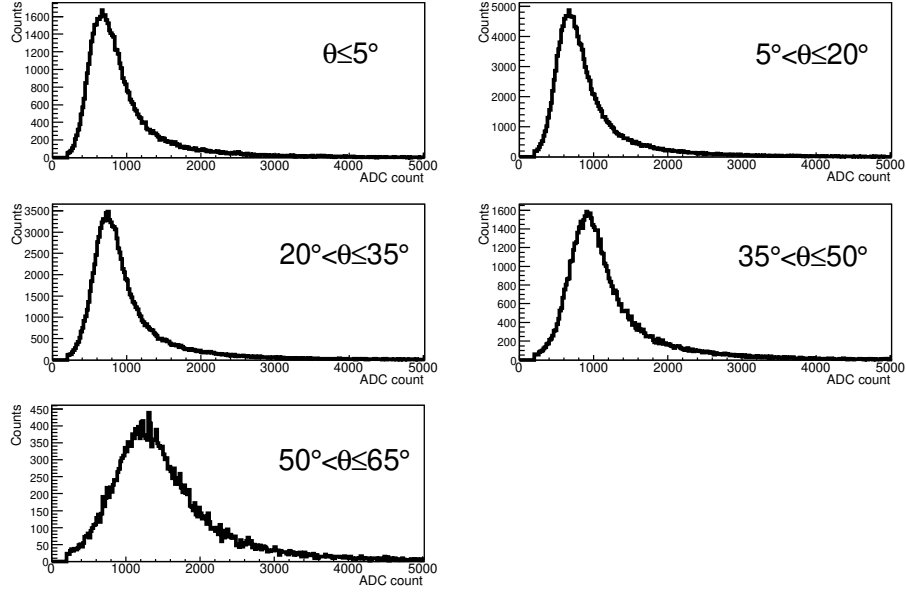


Fig. 15. *In-flight configuration: pull with threshold set to 6 and strip mask ID 6 in physical calibration mode (data acquired with orbit 510) for GRID events with different incidence angles  $\theta$ . The plots contain the data from all the ST planes.*

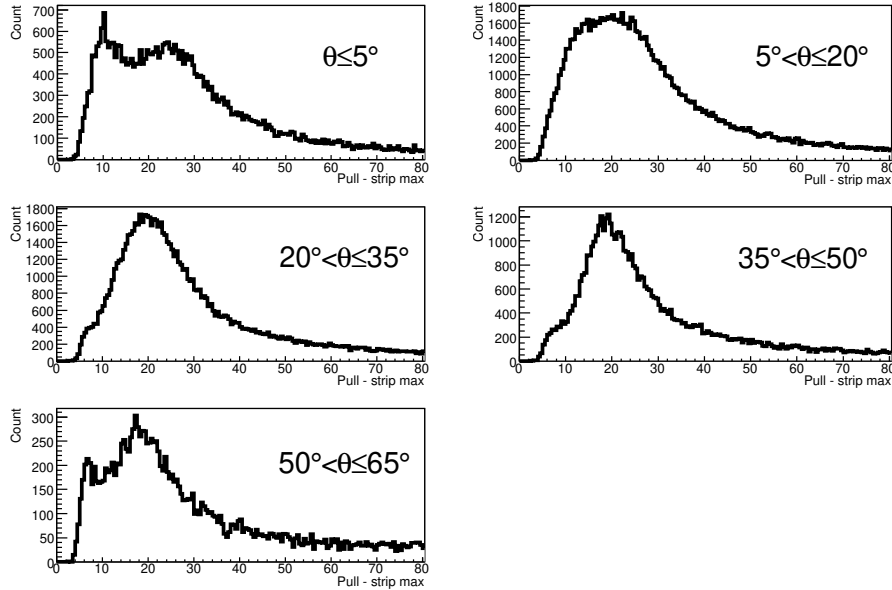


Fig. 16. *In-flight configuration: pull with threshold set to 5 and strip mask ID 7 in physical calibration mode (data acquired with orbit 522) for GRID events with different incidence angles  $\theta$ . The plots contain the data from all the ST planes.*

479 the floating strip is not present, but this Figure, together with the additional  
 480 parameters of the orbit 253 reported in Table 2 has proven that everything  
 481 worked well after the launch.

482 Figure 15 reports a test in physical calibration mode with the FTB thresholds  
 483 set to 6 and the same strip mask defined with the on-ground configuration.

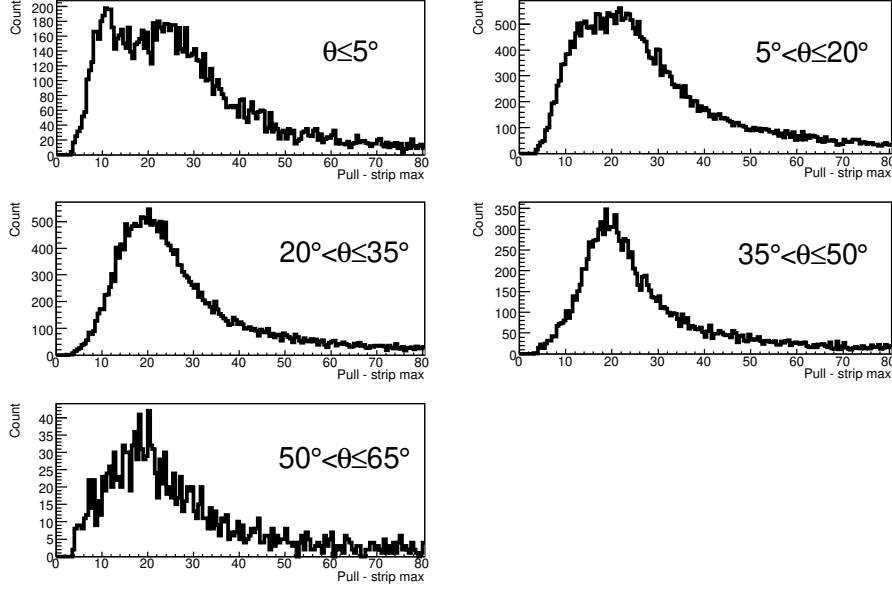


Fig. 17. *In-flight configuration: pull with threshold set to 6 and strip mask ID 8 in physical calibration mode and final strip mask configuration (data acquired with orbit 535) for GRID events with different incidence angles  $\theta$ . The plots contain the data from all the ST planes.*

Table 2

*On-ground (first row) test performed at the end of AIV activities and in-flight test performed during the commissioning phase in May-June 2007 (see Table 1 for a definition of the strip mask identifier): comparative table for GRID physical calibration mode. The orbit 535 has the same configuration of orbit 536.*

Orbit	FTB Thr	Mask ID	Pull X/Z	% event < 3 cl	% $C_3 < 100$ ADC	Eff. X	Eff. Z
RUN 11119	7	6	16.7/16.2 ± 0.2	1.0%	0.0%	95 ± 2%	97 ± 2%
253	20	6	16.7/16.7 ± 0.3	1.5%	0.2%	80 ± 3%	83 ± 2%
510	6	6	18.1/17.4 ± 0.1	5.0%	2.5%	96 ± 1%	97 ± 1%
522	5	7	17.0/17.4 ± 0.2	7.5%	2.5%	96 ± 2%	97 ± 1%
536	6	8	17.2/17.2 ± 0.2	7.0%	2.0%	96 ± 2%	98 ± 2%

484 It is possible to see that with respect to the data acquired on-ground (see  
485 Figure 11) an additional noise peak was present (last plot) in events with  
486 an **incidence angle** greater than 50°: this means that for the higher **inci-**  
487 **dent** **angle** events a **larger fraction of** clusters due to noise are recorded,



Table 3

*In-flight test performed in GRID observation mode during the commissioning phase in May-June 2007 (see Table 1 for a definition of the strip mask identifier): comparative table.*

Orbit	FTB Thr	Mask ID	Pull X/Z	% extra fired	% $C_3 < 100$ ADC	Eff. X	Eff. Z
494	20	6	17.9/17.4±0.2	1.0%	1.0%	84±3%	88±3%
495	10	6	17.8/17.0±0.3	2.0%	1.0%	92±2%	93±2%
507	7	6	17.8/17.0±0.1	6.5%	1.0%	94±2%	95±2%
509	6	6	17.8/17.0±0.2	10.0%	2.0%	95±3%	95±3%
520	6	7	17.7/17.0±0.2	6.6%	2.0%	94±2%	95±1%
523	5	8	18.2/17.0±0.3	11.0%	1.5%	96±2%	95±1%
538	6	8	17.5/17.0±0.2	8.0%	1.0%	96±2%	95±1%

488 a characteristic present only after the launch with this strip mask configu-  
 489 ration; for highly **incidence angle** events the noise peak becomes relatively  
 490 more important with respect to the bulk of particle clusters (because they  
 491 are less) and thus it can be easily identified. To reduce this problem a new  
 492 strip mask (called 7) has been defined and new tests with the orbit 522 have  
 493 been performed (see Figure 16 and Table 2). Due to the time constraint of the  
 494 commissioning phase, also a test with the FTB threshold set to 5 has been  
 495 performed in the same orbit.

496 The final configuration has been reached with orbits 535-536 (see Figure 17  
 497 and Table 2). For a better stability of the system during the nominal phase a  
 498 threshold of 6 has been chosen with the strip mask indicated with 8 with 665  
 499 disabled strips corresponding to 1.8% of the overall Silicon Tracker channels.  
 500 A test in the GRID observation mode has been performed with the same con-  
 501 figuration used in the physical calibration mode. The main results are reported  
 502 in Table 3.

503 It is important to note the progressive trend towards improving of the in-flight  
 504 ST configuration. In particular, the quite high values of the overall ST detec-  
 505 tion and trigger efficiency (95-96 %) have to be underlined. Considering the  
 506 peculiar AGILE ST working and readout system based on analog signals, these  
 507 **high efficiencies** are very important for an optimal scientific performance of

508 the instrument.

## 509 **10 Conclusions**

510 This paper presents the main results of the extensive testing campaigns of the  
511 AGILE Silicon Tracker electronic configuration. The ST has been configured  
512 in different steps, and **it** reached an optimal performance during the pre-  
513 launch and post-launch tests. After almost 2 years of in-orbit operations the  
514 ST configuration that was consolidated during the commissioning phase is  
515 quite stable. Additional noisy strips (about 20) have been identified during  
516 the day-by-day data observations **in** the first 2 years with a negligible effect  
517 on the overall performance. The AGILE Silicon Tracker, that is the heart of  
518 the instrument, is then optimally configured and its digital readout system is  
519 remarkably stable for scientific observations in space.

## 520 **Acknowledgments**

521 The AGILE Mission is funded by the Italian Space Agency (ASI) with scien-  
522 tific and programmatic participation by the Italian Institute of Astrophysics  
523 (INAF) and the Italian Institute of Nuclear Physics (INFN). The authors wish  
524 to thank all the AGILE team for their help and fruitful discussions. The au-  
525 thors wish to thank also the industrial partners, namely the AGILE people at  
526 Thales-Alenia Space Italia and Carlo Gavazzi Space.

## 527 **References**

- 528 [1] M. Tavani et al., *Astron. Astrophys.* 520 (2009) 995-1013
- 529 [2] G. Barbiellini et al., *Nucl. Instr. and Meth. A* 490 (2002) 146-158
- 530 [3] M. Prest et al., *Nucl. Instr. and Meth. A* 501 (2003) 280-287
- 531 [4] M. Feroci et al., *Nucl. Instr. and Meth. A* 581 (2007) 728-754
- 532 [5] C. Labanti et al., *Nuclear Physics B Proc. Suppl.* 150 (2006) 34-37
- 533 [6] F. Perotti et al., *Nucl. Instr. and Meth. A* 556 (2006) 228-236
- 534 [7] M. Basset et al., *Proc. Third Workshop on Science with the New Generation*  
535 *of High Energy Gamma-ray Experiments, Cividale del Friuli, Italy, 2006*

- 536 [8] C. Pontoni, M. Prest, E. Vallazza, The AGILE Silicon Tracker: technical  
537 requirements for the FTB and the MLC, INFN Internal Report, AGILE-ITS-  
538 SS-001, 27/12/2000
- 539 [9] A. Argan et al., Proc. IEEE Nuclear Science Symposium Conference Record,  
540 vol. 1, 16-22 October, 2004, IEEE, pp. 371-375
- 541 [10] M. Prest et al., Nucl. Instr. and. Meth. A 501 (2002) 280-287
- 542 [11] F. Gianotti, M. Trifoglio, Proc. ADASS X, ASP Conf. Ser. 238 (2001) 238-245
- 543 [12] A. Bulgarelli et al., Proc. ADASS XII, ASP Conf. Ser. 295 (2003) 473-476
- 544 [13] M. Trifoglio et al., Proc. SPIE 7011 (2008)
- 545 [14] A. Bulgarelli et al., Proc. SPIE 7011 (2008)